



# Straightforward method to measure optomechanically induced transparency

F. M. BUTERS,<sup>1,\*</sup> F. LUNA,<sup>2</sup> M. J. WEAVER,<sup>2</sup> H. J. EERKENS,<sup>1</sup> K. HEECK,<sup>1</sup> S. DE MAN,<sup>1</sup> AND D. BOUWMEESTER<sup>1,2</sup>

<sup>1</sup>*Huygens-Kamerlingh Onnes Laboratorium, Universiteit Leiden, 2333 CA Leiden, The Netherlands*

<sup>2</sup>*Department of Physics, University of California, Santa Barbara, CA 93106, USA*

\**buters@physics.leidenuniv.nl*

**Abstract:** We demonstrate a simple method to measure optomechanically induced transparency (OMIT) in a Fabry-Perot based system using a trampoline resonator. In OMIT, the transmitted intensity of a weak probe beam in the presence of a strong control beam is modified via the optomechanical interaction, leading to an ultra-narrow optical resonance. To retrieve both the magnitude and the phase of the probe beam, a homodyne detection technique is typically used. We have greatly simplified this method by using a single acousto-optical modulator to create a control and two probe beams. The beat signal between the transmitted control and probe beams shows directly the typical OMIT characteristics. This method therefore demonstrates an elegant solution when a homodyne field is needed but experimentally not accessible.

© 2017 Optical Society of America

OCIS codes: (200.4880) Optomechanics; (190.4223) Nonlinear wave mixing.

## References and links

1. M. Aspelmeyer, T.J. Kippenberg, and F. Marquardt, "Cavity optomechanics," *Rev. Mod. Phys.* **86**(4), 1391 (2014).
2. V. Fiore, Y. Yang, M.C. Kuzyk, R. Barbour, L. Tian, and H. Wang, "Storing optical information as a mechanical excitation in a silica optomechanical resonator," *Phys. Rev. Lett.* **107**(13), 133601 (2011).
3. J. T. Hill, A. H. Safavi-Naeini, J. Chan, and O. Painter, "Coherent optical wavelength conversion via cavity optomechanics," *Nature Communications* **3**(13), 1196 (2012).
4. A. H. Safavi-Naeini, T. M. Allegrè, J. Chan, M. Eichenfield, M. Winger, Q. Lin, J. T. Hill, D. E. Chang, and O. Painter, "Electromagnetically induced transparency and slow light with optomechanics," *Nature* **472**(7341), 69–73 (2011).
5. K. -J. Boller, A. Imamoglu, and S. E. Harris, "Observation of electromagnetically induced transparency," *Phys. Rev. Lett.* **66**(20), 2593 (1991).
6. L. V. Hau, S. E. Harris, Z. Dutton, and C. H. Behroozi, "Light speed reduction to 17 metres per second in an ultracold atomic gas," *Nature* **397**(594), 594–598 (1999).
7. S. Weis, R. Rivière, S. Deléglise, E. Gavartin, O. Arcizet, A. Schliesser, and T. J. Kippenberg, "Optomechanically induced transparency," *Science* **330**(6010), 1520–1523 (2010).
8. J. Teufel, D. Li, M. Allman, K. Cicak, A. Sirois, J. Whittaker, and R. Simmonds, "Circuit cavity electromechanics in the strong-coupling regime," *Nature* **471**(7337), 204–208 (2011).
9. M. Karuza, G. Biancofiore, M. Bawaj, C. Molinelli, M. Galassi, R. Natali, P. Tombesi, G. Di Giuseppe, and D. Vitali, "Optomechanically induced transparency in a membrane-in-the-middle setup at room temperature," *Phys. Rev. A* **88**(1), 013804 (2013).
10. J. Qin, C. Zhao, Y. Ma, X. Chen, L. Ju, and D. G. Blair, "Classical demonstration of frequency-dependent noise ellipse rotation using optomechanically induced transparency," *Phys. Rev. A* **89**(4), 041802 (2014).
11. W. H. P. Nielsen, Y. Tsaturyan, C. B. Møller, E. S. Polzik and A. Schliesser, "Multimode optomechanical system in the quantum regime," *Proceedings of the National Academy of Sciences*, 201608412 (2016).
12. G. Agarwal and S. Huang, "Electromagnetically induced transparency in mechanical effects of light," *Phys. Rev. A* **81**(4), 041803 (2010).
13. H. Eerkens, F. Buters, M. Weaver, B. Pepper, G. Welker, K. Heeck, P. Sonin, S. de Man, and D. Bouwmeester, "Optical side-band cooling of a low frequency optomechanical system," *Opt. Express* **23**(6), 8014–8020 (2015).
14. E. D. Black, "An introduction to Pound–Drever–Hall laser frequency stabilization," *American Journal of Physics* **69**(1), 79–87 (2001).
15. M. J. Weaver, B. Pepper, F. Luna, F. M. Buters, H. J. Eerkens, G. Welker, B. Perock, K. Heeck, S. de Man, and D. Bouwmeester, "Nested Trampoline Resonators for Optomechanics," *Appl. Phys. Lett.* **108**, 033501 (2016).
16. R. W. Boyd and D. J. Gauthier, "Controlling the velocity of light pulses," *Science* **326**(5956), 1074–1077 (2009).

## 1. Introduction

Cavity optomechanics has attracted much attention recently, see Ref. [1] for an overview. This attention is partly due to the prospect of performing experiments involving non-classical states of a macroscopically sized object. Such experiments typically overcome the thermal mechanical motion by preparing the system in the quantum mechanical ground state. For applications such as light storage [2], optical wavelength conversion [3] and delay lines [4], ground state cooling is not a strict requirement. For example, an optomechanical delay line can be constructed around the effect of optomechanically induced transparency or OMIT, the optomechanical equivalent to electromagnetically induced transparency (EIT) [5, 6] in atomic systems. This effect is achieved by driving the system with two tones, a control and probe beam, and has been demonstrated by several groups [7–11], showing that OMIT has become a powerful tool to characterize optomechanical systems. Consequently, different measurement schemes have been used to perform these measurements. Here we demonstrate a straightforward, easy to implement method to perform OMIT, together with a detailed model to analyze the data. Our method is not restricted to a particular optomechanical system, nor does it require to be in the side-band resolved regime.

Using a membrane-in-the-middle set-up, Karuza et al. have shown how the transmitted control beam can be used as a phase reference to perform a modified heterodyne detection technique [9]. Here we expand on this idea by measuring the beat signal from the control and probe beam, but instead of using multiple acoustic-optical modulators (AOMs), we use a single AOM to create a control and two probe beams via double side-band generation. Although a similar experiment has been performed using a single electro-optical modulator (EOM) [11], we provide significantly more theoretical and experimental details. For example, the presence of two probes instead of one requires modification of the OMIT theory as we will show below.

This method is especially advantageous with low mechanical frequency systems. The typical frequency difference between pump and probe beam is between 100 kHz and 1 MHz for such systems. The OMIT feature itself however, is of the order of the mechanical linewidth [12]. Therefore the laser frequencies involved, need to be set with high precision. This can best be accomplished using a lock-in amplifier. The reference frequency output of the lock-in amplifier modulates the RF drive to the AOM to generate the pump and two probes, while the transmitted intensity is recorded with the same lock-in amplifier. In this way the change in probe detuning can not only be monitored with sub-Hz precision, but the common path of both control and probe beams greatly increases the stability of the experiment.

First, we briefly describe the OMIT theory and show the modifications needed for the two probe measurements. After the experimental details, we show how the typical OMIT features, namely an ultra-narrow optical resonance, are recorded by independently controlling both control and probe beam, something which was not possible in the work of Karuza et al. Finally, the results are compared with theory. We find a good agreement and are able to reduce the transmitted intensity of the probe beam by more than 4 orders of magnitude, resulting in a final optomechanical cooperativity of  $144 \pm 5$ .

## 2. Theory

A detailed theory for OMIT can be found in the work by Agarwal et al. [12]. A short summary is given by Aspelmeyer et al. [1] of which we will repeat the key points.

The principle of OMIT is the following: a strong control beam is placed on the lower side-band at a laser detuning of  $\Delta = -\Omega_m$ , where  $\Omega_m$  is the frequency of the mechanical resonator. A second, weak, probe beam is placed at the cavity resonance, such that the mechanical resonator is driven by the two photon interaction with both probe and control beam. This is schematically depicted in Fig. 1(a). The strongly driven mechanical resonator modulates the control beam and creates Stokes and anti-Stokes side-bands, indicated in blue in Fig. 1(a). The interference between

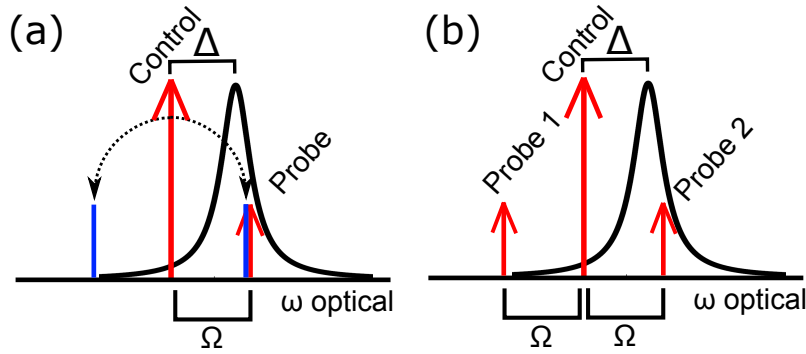


Fig. 1. Schematic overview of the placement and relative location for the control and probe beam.  $\Delta$  indicates the detuning of the control beam with respect to the cavity resonance, and  $\Omega$  is the probe detuning with respect to the control beam (a) The case with only a single probe. The two blue lines indicate the Stokes and anti-Stokes side-bands generated via the optomechanical interaction. (b) The case presented in this work, where two probes are used.

side-band and probe beam reduces the amplitude and changes the phase of the transmitted probe beam. The dispersive behavior of the transmitted probe beam results in a change in group velocity and can be viewed as a delay of the propagating beam.

For a Fabry-Perot based system, the field of a single transmitted probe in the presence of a strong control beam is given by the following expression:

$$t_p = \eta\kappa \frac{\chi_{aa}(\Omega)}{1 + g^2 \chi_{mech}(\Omega) \chi_{aa}(\Omega)} \quad (1)$$

with the following parameters:  $\eta = \frac{\kappa_{ex}}{\kappa}$  is the coupling efficiency,  $\kappa$  is the cavity linewidth,  $\kappa_{ex}$  is the input coupling rate,  $\Gamma_m$  is the mechanical linewidth,  $g$  is the optomechanical multi-photon coupling rate,  $\chi_{aa}(\Omega)$  is the optical susceptibility defined as  $\chi_{aa}^{-1}(\Omega) = -i(\Omega + \Delta) + \kappa/2$  and  $\chi_{mech}(\Omega)$  is the mechanical susceptibility defined as  $\chi_{mech}^{-1}(\Omega) = -i(\Omega - \Omega_m) + \Gamma_m/2$ . We have introduced the detuning of the control beam as  $\Delta = \omega_{control} - \omega_{cavity}$  and the detuning of the probe beam as  $\Omega = \omega_{probe} - \omega_{control}$ . Note that compared to some previous work [4, 7], we use a Fabry-Perot based system. When measuring the transmitted probe, instead of a transparency window a dark window will appear. Effectively the transmission and reflection signals are exchanged when comparing a Fabry-Perot system with a waveguide coupled cavity. We will however still refer to an OMIT feature to be consistent with existing literature.

In our experiment the transmitted intensity of two probes spaced symmetrically around the control beam is measured, see Fig. 1(b). In the side-band resolved regime, where  $\kappa \ll \Omega_m$ , probe 1 can be ignored. The experiment presented here operates in the regime where  $\kappa \approx \Omega_m$ , so a portion of probe 1 is still transmitted and the presence of this probe beam cannot be ignored. To accurately describe the experiment, Eq. (1) is modified in the following way (see appendix):

$$t_p = \eta\kappa \frac{2\chi_{aa}(\Omega) [-i + \chi_{aa}(\Omega)\Omega]}{-i + 2\chi_{aa}(\Omega)\Omega [1 + g^2 \chi_{mech}(\Omega) \chi_{aa}(\Omega)]}. \quad (2)$$

The transmitted intensity is obtained via  $|t_p|^2$ .

The transmitted intensity for both the single probe (blue) and two probes (red) are shown in Fig. 2, for  $\Delta = -\Omega_m$  and  $\Omega_m = 1.6\kappa$  while varying the probe detuning  $\Omega$ . The presence of the two probes modifies the OMIT feature slightly, but this effect becomes smaller when the ratio  $\Omega_m/\kappa$  increases. Note that the typical OMIT dip is still nicely visible when using two

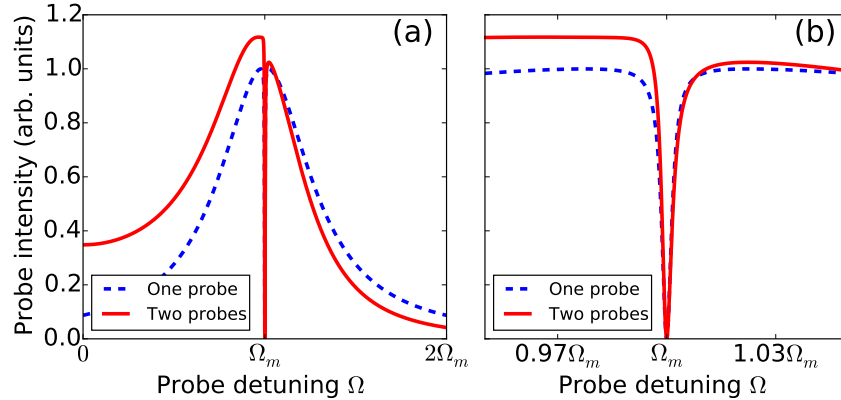


Fig. 2. (a) Comparison of OMIT feature for one transmitted probe (blue) and two transmitted probes (red) with  $\Omega_m = 1.6\kappa$ . The control beam is placed at  $\Delta = -\Omega_m$  and the probe detuning  $\Omega$  is varied. (b) Close-up of the OMIT feature.

probes. This is important because from this dip both the total effective damping rate  $\Gamma_{eff}$  and the multi-photon cooperativity  $C = 4g^2/\kappa\Gamma_m$  can be extracted. A convenient way to do this, is to measure the transmitted intensity on resonance, i.e. with  $\Delta = -\Omega_m$  and  $\Omega = \Omega_m$ , which is given by

$$|t_p|^2 = \left( \frac{2\eta}{1+C} \right)^2 \left| 1 + \frac{1+2C}{1+i4(1+C)\Omega_m/\kappa} \right|^2. \quad (3)$$

In the sideband resolved limit,  $\kappa \ll \Omega_m$ , this reduces to the familiar expression [4, 7]:

$$|t_p|^2 = \left( \frac{2\eta}{1+C} \right)^2. \quad (4)$$

Finally, not only the magnitude of the transmitted probe but also the phase of the probe changes when varying the probe detuning. The dispersive behavior of the transmitted probe beam leads to a group delay. The argument of Eq. (2) gives the phase of the probe and the group delay is obtained by taking the derivative of the phase:

$$\tau_g = \frac{d\phi}{d\Omega} \quad (5)$$

For  $\Delta = -\Omega_m$ ,  $\Omega = \Omega_m$  and assuming  $\kappa \gg \Gamma_m$  the group delay is given by

$$\tau_g = -\frac{2}{\Gamma_m} \left( \frac{C}{C+1} \right) \left( 1 + \frac{1}{1+16(1+C)^2\Omega_m^2/\kappa^2} \right). \quad (6)$$

which in the limit for  $C \gg 1$  results in  $\tau_g = -\frac{2}{\Gamma_m}$ . Both the magnitude and the phase of the OMIT feature can therefore be used to derive the system parameter  $C$ .

### 3. Experimental details

Our optomechanical system consist of a 5 cm long Fabry-Perot cavity with a trampoline resonator as one of the end mirrors. As mentioned before we use a single AOM to generate a control and two probe beams. To eliminate cavity or laser drift we use the scheme outlined in Eerkens et al. [13]. One laser (Laser 1 in Fig. 3) is locked to the cavity resonance via the Pound-Drever-Hall

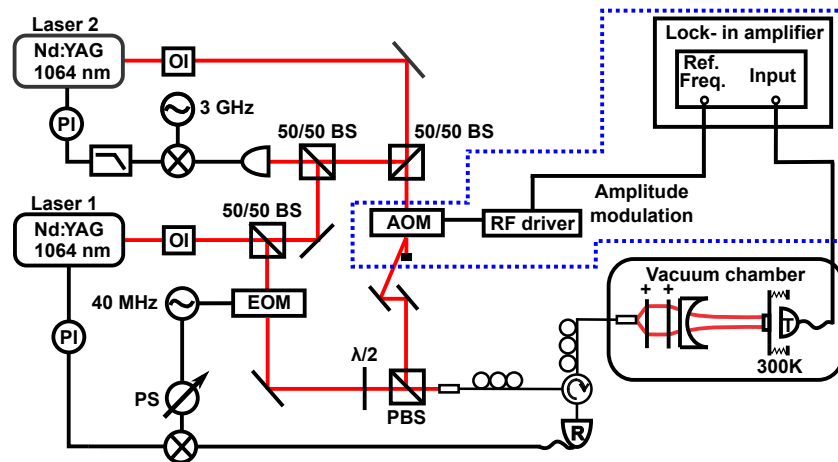


Fig. 3. Experimental set-up. This is a modified version of the set-up presented by Eerkens et al. [13]. The additional components needed to measure OMIT are highlighted with the dashed blue line. The RF drive signal to the AOM is modulated at the reference frequency of the lock-in amplifier to create a control and two probe beams. The transmitted intensity of the control and probe beams is analyzed using the lock-in amplifier. The components displayed are: LO: local oscillator, BS: beam splitter, PBS: polarizing beam splitter, EOM: electro-optical modulator, OI: optical isolator and PI: proportional-integral feedback controller

(PDH) technique [14]. This laser serves purely as a reference and is not used to read out the motion of the resonator. A second laser (Laser 2 in Fig. 3) is, with a variable frequency offset, locked to the first laser one free spectral range away using an optical phase locked loop. From this second laser the control and probe beams are derived. An overview of the experimental set-up is presented in Fig. 3. To be able to measure OMIT, our existing set-up is expanded to include an AOM and lock-in amplifier. These components are highlighted with the blue dashed line. The lock-in amplifier is used to modulate the RF drive to the AOM, generating two probes via double sideband generation. By adjusting the modulation frequency, the detuning of the probe beams is set. The power of the control beam is adjusted by changing the magnitude of the RF drive to the AOM, while the power of the probe beams is adjusted by changing the amplitude of the modulation. Typically only a few  $\mu\text{W}$  of optical power is used for the probe beams, while the power of the control beam can be varied separately. The transmitted intensity is recorded using a photodetector and analyzed using the same lock-in amplifier to obtain both phase and amplitude of the transmitted probes.

The measurements are performed using a nested trampoline resonator [15]. The optical and mechanical properties of the system are characterized separately. Via an optical cooling experiment (see Ref. [13]) the optical linewidth is determined to be  $185 \pm 4$  kHz. Based on the reflected and transmitted intensity, the coupling efficiency  $\eta$  is estimated to be 0.3. The mechanical resonator is characterized by measuring its mechanical thermal noise spectrum with a side-of-fringe lock to a low finesse cavity. An intrinsic mechanical linewidth of  $\Gamma_m = 30 \pm 0.1$  Hz and a mechanical frequency of 291.8 kHz was obtained. The mode-mass of the resonator is, via COMSOL, estimated to be 180 ng. Although these parameters are relatively modest compared to our previous work (see Ref. [15]), they suffice for demonstrating optomechanically induced transparency.

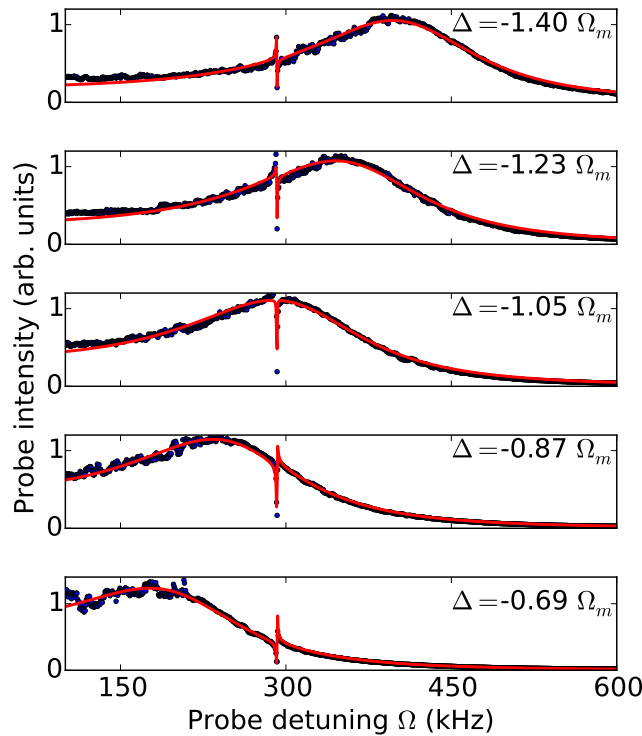


Fig. 4. Demonstration of optomechanical induced transparency. The probe detuning  $\Omega$  is varied for different values of the pump detuning  $\Delta$ .

#### 4. Results

To demonstrate optomechanically induced transparency, the probe intensity and phase are recorded while the probe detuning  $\Omega$  is varied. In Fig. 4 the results are shown for five different pump detunings  $\Delta$ . Regardless of the pump detuning, a significant dip in probe intensity always occurs for a probe detuning  $\Omega = \Omega_m$ . This is a key feature of OMIT. Experiment and theory are in good agreement, as evidenced by the fitted red line using Eq. (2). For the fit three free parameters are used: pump detuning  $\Delta$ , optical linewidth  $\kappa$  and pump laser power. The value for the optical linewidth,  $193 \pm 4$  kHz, is in agreement with the separate characterization of the set-up.

To investigate the OMIT feature in more detail, the control beam is set at  $\Delta = -\Omega_m$  and the probe detuning is varied around  $\Omega \approx \Omega_m$ . The effect of pump power is shown in Fig. 5. The top two panels show the intensity of the transmitted probe and the intensity of the transmitted probe on resonance. The transmitted probe intensity can be changed more than four orders of magnitude by varying the power of the control beam. The bottom panels show the phase of the transmitted probe and the group delay derived from the derivative of the phase, see Eq. (5). The dashed line is the theoretical minimum set by  $-2/\Gamma_m$ . Note that a negative group delay suggests a superluminal group velocity, an effect which has been studied extensively in the past (see Ref. [16] for an overview). Both the transmission on resonance and group delay can be fitted using Eqs. (3) and (6) to obtain the optomechanical cooperativity for each control beam power. For the highest laser power a maximum cooperativity of  $144 \pm 5$  is achieved.

We can also achieve optomechanically induced amplification by setting the detuning of the control beam to  $\Delta = +\Omega_m$ . Note that the system is only stable when the effective mechanical

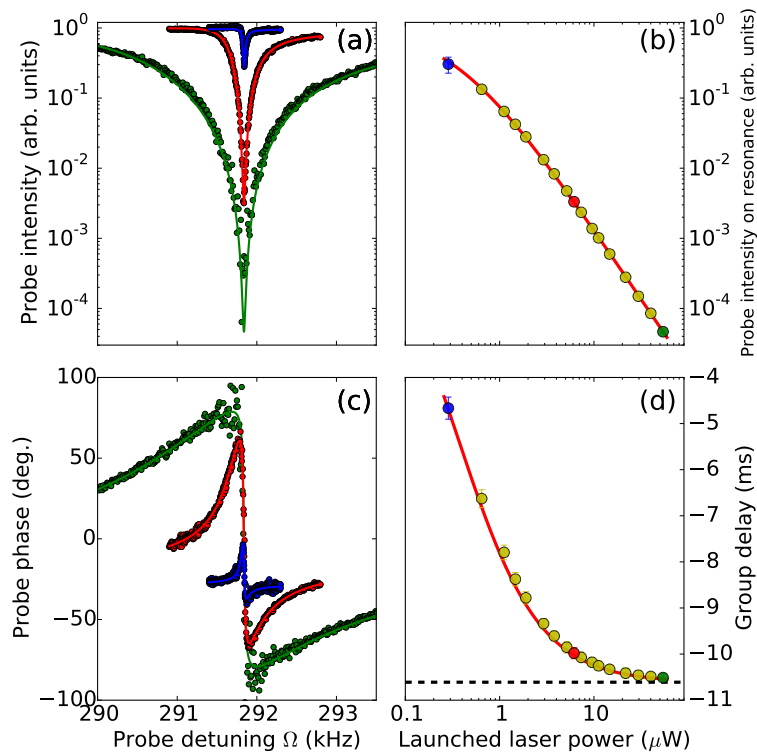


Fig. 5. For a fixed control detuning of  $\Delta = -\Omega_m$  the control beam power is varied. (a) The transparency window increases with laser power. (b) Transmitted probe intensity on resonance. (c) Phase of the transmitted probe. (d) Group delay obtained via the derivative of the phase.

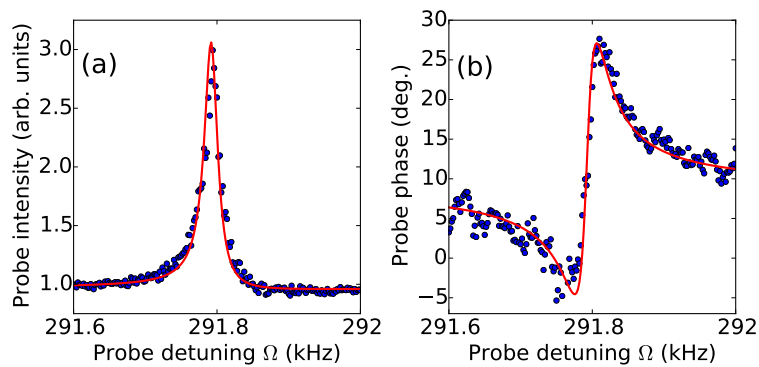


Fig. 6. Demonstration of optomechanically induced amplification by placing the pump at  $\Delta = +\Omega_m$ . (a) Transmitted probe intensity (b) Phase of transmitted probe.

damping is still positive, which requires  $C < 0.5$  when critical coupling is assumed. Increasing the control beam power further leads to parametric amplification of the mechanical mode. The result of a blue detuned control beam is shown in Fig. 6. Now an increase in transmitted probe together with a positive group delay of 5.9 ms is achieved. Comparing this delay to the cavity lifetime shows that the delay has increased with a factor of 3700. As before, the maximum delay is limited to  $2/\Gamma_m = 10.6$  ms. Increasing the mechanical quality factor will create a longer delay, but this requires also careful adjustment of the control beam power to stay below the threshold for parametric amplification. However, a delay of 5.9 ms is already significant; more than 1000 km of fiber is needed to achieve the same effect.

As demonstrated above, all the typical OMIT features are reproduced using the method with two probe beams. Furthermore, the increased stability of the common path of both local oscillator and signal is beneficial for a wide variety of experiments. Finally, for some experimental configurations the implementation of a homodyne/heterodyne detection scheme is technically not possible. The method presented in this work is an elegant solution to this problem.

## 5. Conclusion

In conclusion, we have presented a simple and straightforward method to measure optomechanically induced transparency. Using a single AOM and lock-in amplifier, OMIT can easily be measured with full control and high precision of both control and probe detuning. The working principle is demonstrated using a relatively modest optomechanical system in terms of system parameters, making this method applicable to a wide variety of systems. Furthermore, the modified heterodyne technique demonstrated here as well as the generation of multiple tones via a single AOM can be applied to a variety of experiments within the field of optomechanics.

### Derivation of the transmission with two probes

Here we briefly show how Eq. (2) is derived using an approach similar to Weis et al. [7]. The classical optomechanical equations (in the rotating frame) are the following:

$$\frac{da(t)}{dt} = (i(\Delta + Gx(t)) - \frac{\kappa}{2})a(t) + \sqrt{\eta\kappa}s_{in}(t) \quad (7)$$

$$\frac{d^2x(t)}{dt^2} = -\Gamma_m \frac{dx(t)}{dt} - \Omega_m^2 x(t) + \frac{\hbar G}{m} |a(t)|^2 \quad (8)$$

in which  $a(t)$  is the optical field inside the cavity,  $G$  the optical frequency shift per displacement,  $x(t)$  the mechanical displacement and  $s_{in}(t)$  the input field.

The motion of the harmonic oscillator can be treated as a small perturbation around some mean displacement:  $x(t) = \bar{x} + \delta x(t)$ . Similarly the effect of this motion on the cavity field can be treated as a perturbation:  $a(t) = \bar{a} + \delta a(t)$ . Substituting these assumptions in Eqs. (7) and (8) yields:

$$\frac{d\delta a(t)}{dt} = (i[\Delta + G(\bar{x} + \delta x(t))] - \frac{\kappa}{2})(\bar{a} + \delta a(t)) + \sqrt{\eta\kappa}(\bar{s}_{in} + \delta s_{in}(t)) \quad (9)$$

$$\frac{d^2\delta x(t)}{dt^2} = -\Gamma_m \frac{d\delta x(t)}{dt} - \Omega_m^2(\bar{x} + \delta x(t)) + \frac{\hbar G}{m} [(\bar{a} + \delta a(t))(\bar{a}^* + \delta a^*(t))] \quad (10)$$

Setting  $\delta a(t) = 0$  and  $\delta x(t) = 0$  results in the following steady state solution:

$$\bar{a} = \frac{\sqrt{\eta\kappa}\bar{s}_{in}}{i(\Delta + G\bar{x}) - \kappa/2} \quad (11)$$

$$\bar{x} = \frac{\hbar G}{m\Omega_m^2} |\bar{a}|^2. \quad (12)$$



Inserting the steady state solution back in Eqs. (9) and (10) leads to the following equations for  $\delta x(t)$  and  $\delta a(t)$ :

$$\frac{d\delta a(t)}{dt} = (i\Delta - \frac{\kappa}{2})\delta a(t) + iG\bar{a}\delta x(t) + \delta s_{in}(t) \quad (13)$$

$$\frac{d^2\delta x(t)}{dt^2} = -\Gamma_m \frac{d\delta x(t)}{dt} - \Omega_m^2 \delta x(t) + \frac{\hbar G\bar{a}}{m} [\delta a(t) + \delta a^*(t)] \quad (14)$$

Note that we have dropped second-order terms and assumed that the static radiation pressure is negligible.

Instead of a single probe as the input, we now have two probes at frequencies  $\pm\Omega$ , therefore  $\delta s_{in}(t) = s_p (e^{-i\Omega t} + e^{+i\Omega t})$ . As an ansatz to solve Eqs. (13) and (14) we use the following:

$$\delta a(t) = A^- e^{-i\Omega t} + A^+ e^{+i\Omega t} \quad (15)$$

$$\delta a^*(t) = (A^+)^* e^{-i\Omega t} + (A^-)^* e^{+i\Omega t} \quad (16)$$

$$\delta x(t) = X e^{-i\Omega t} + X^* e^{+i\Omega t}. \quad (17)$$

Inserting the drive  $\delta s_{in}(t)$  and the ansatz back in Eqs. (13 - 14), and solving for  $A^-$  and  $A^+$  results in:

$$A^+ = s_p \sqrt{\eta\kappa} \frac{\chi_{aa}(\Omega) [i - 2\chi_{aa}(\Omega)\Omega]}{-i + 2\chi_{aa}(\Omega)\Omega [1 + g^2\chi_{mech}(\Omega)\chi_{aa}(\Omega)]} \quad (18)$$

$$A^- = s_p \sqrt{\eta\kappa} \frac{i\chi_{aa}(\Omega)}{-i + 2\chi_{aa}(\Omega)\Omega [1 + g^2\chi_{mech}(\Omega)\chi_{aa}(\Omega)]}. \quad (19)$$

This is the resulting field for each probe inside the cavity. In the end we measure, via the beat with the control beam, the coherent sum of the two transmitted probes, therefore:

$$t_p = \frac{\sqrt{\eta\kappa}}{s_p} [A^+ + A^-] \quad (20)$$

which after some manipulation leads to Eq. (2).

In the presence of additional optical losses, defined as  $\kappa_{loss}$ , the transmitted probe of Eq. 20 becomes:

$$t_p = \frac{\eta\kappa}{s_p(\sqrt{\eta\kappa} + \sqrt{\kappa_{loss}})} [A^+ + A^-] \quad (21)$$

## Funding

Netherlands Organisation for Scientific Research (NWO); National Science Foundation (PHY-1212483).

## Acknowledgments

This work is part of the research program of the Foundation for Fundamental Research (FOM) and of the NWO VICI research program, which are both part of the Netherlands Organisation for Scientific Research (NWO).

The authors would like to thank H. van der Meer for technical assistance. The authors are also grateful for useful discussions with W. Loeffler.